VNU Journal of Science: Mathematics – Physics, Vol. 39, No. 2 (2023) 56-65

VNU Journal of Science: Mathematics - Physics

Journal homepage: https://js.vnu.edu.vn/MaP

Original Article

Optimization of Dispersions in GeO_2-doped Photonic Crystal Fibers with Square Lattice

Nguyen Thi Thuy*

University of Education, Hue University, 34 Le Loi, Hue City, Vietnam

Received 29 October 2022
Revised 26 December 2022; Accepted 27 February 2023

Abstract: Germanium doped photonic crystal fibers with differences in the layers' air hole diameters in the cladding are presented to obtain flat dispersion, small effective mode area, and low attenuation property for supercontinuum generation applications. The flatness and small value of the dispersion depend on the lattice geometry when the fibers have the same germanium doping concentration. The dispersion of the square lattice fibers is a flatter and smaller value at the pump wavelength than the circular lattice fibers. Square lattice fibers with Λ = 0.9 µm, d_1/Λ = 0.4 and Λ = 1.0 µm, d_1/Λ = 0.45 are proposed for supercontinuum generation which has anomalous and all-normal dispersion, respectively. Their small dispersion values of 0.449 ps /nm.km and −1.096 ps/nm.km are suitable for broad spectrum supercontinuum generation. The small effective mode area and low attenuation of the two fibers of 3.221 µm^2, 2.361 µm^2 and 1.805×10^{-7} dB/m, 1.322×10^{-15} dB/m, respectively are favorable conditions for choosing a laser pump sources with low peak power. The proposed fibers can be new supercontinuum generation source replacing traditional glass core fibers.

Keywords: Photonic crystal fibers, germanium, flat dispersion, small effective area, low attenuation.

1. Introduction

With flexibility in structural design, photonic crystal fibers (PCFs) are a potential medium for many applications, especially in supercontinuum generation (SC). Owing to the excellent thermomechanical properties and maturity of fabrication technology, silica-based fibers appear to be the most natural choice. However, pure silica has high phonon energy, about 1100 cm^{-1} [1], which limits the SC spectrum expansion in the mid-infrared region wavelength. To overcome this limitation, many solutions in SiO_2-

* Corresponding author.
E-mail address: ntthuy@hueuni.edu.vn

https//doi.org/10.25073/2588-1124/vnumap.4787

based fiber design have been shown to improve dispersion, and enhance fiber nonlinearity, i.e. improve SC transmission efficiency.

Filling the hollow cores or air holes in the cladding with highly nonlinear fluids improves the fibers' dispersion and nonlinear properties, which have attracted current research groups. The flat dispersions and small pump wavelength help to broaden the SC spectrum when the fiber is injected in the all-normal or anomalous dispersion region [2-8]. Furthermore, the characteristic quantities of these PCFs, such as small effective mode area, high nonlinear coefficient, and low loss reduce the peak power of the pump source, which improves the SC generation efficiency.

Using substances with high nonlinearity and low phonon energy such as GeO_2 to dope into the cores of SiO_2-PCFs with a certain molar concentration is also an excellent solution to diversify the application field and improve SC efficiency [9-11]. Depending on the doping concentration, the fibers can give losses lower than 120 dB/km at 1.9–2.0 µm [12]. A flat normal dispersion in the wavelength region of 1.2–2.1 µm was achieved in SiO_2-PCFs using doped GeO_2 [13]. The coherent SC spectrum was generated through PCFs with dispersion as small as − 0.3 to 0 ps/(nm.km) in the wavelength region of 1.49–1.85 µm [14]. The nonlinear coefficient of 83 $W^{-1}.km^{-1}$ at 1.55 µm was obtained by designing GeO_2-doped PCFs with a core refractive index higher than 3% [15]. GeO_2-doped PCFs with octagonal structure exhibited nonlinearity as high as 4,500 $W^{-1}.km^{-1}$ at 1,000 nm and confinement loss as low as 10^{-9} dB/m at 1,800 nm [16]. The flatness and value of the dispersion can be controlled through adjustment of the GeO_2 doping concentration, the authors [17] achieved a nonlinear coefficient of 0.0166 $W^{-1}.m^{-1}$ and a small dispersion of −11.8 ps/(nm.km) at 1.55 µm, beneficial for wideband supercontinuum generation.

Although the damage threshold of GeO_2 is low (fews orders of magnitude lower than that of silica) [18], GeO_2-doped PCFs have been experimentally fabricated to obtain broad-spectrum SC at different pumping wavelengths [19, 20]. The experiments reported in [21] proved a highest output power for a broadest spectrum from 700 nm to 3,200 nm based on GeO_2-doped PCF at 1.55 m pump wavelength.

In this work, we compare the dispersion of PCFs with a GeO_2-doped core with the same molar concentration but a different lattice structure. With a 10 mol% of GeO^2, fibers with square lattice give smaller and flatter dispersion than circular lattice fibers. Based on the numerical analysis results, two fibers with optimal dispersion are proposed for SC generation application. Furthermore, the low attenuation of about 10^{-7} dB/m and the small effective mode area of a few µm^2 are favorable factors for selecting SC generation with low peak power.

2. Numerical Modeling of the PCFs

The structural geometric cross-sections of square and circular lattice GeO_2-doped PCFs are shown in Fig. 1. We used Lumerical Mode Solution (LMS) software to simulate the structure of PCFs with square and circular lattice structures. The square and circular lattice structures are designed with six layers of air holes in the cladding. They are regularly arranged around the core spaced apart (Λ = 0.9 µm and 1.0 µm). The diameter d_2 of the air holes in the second layer is designed differently from the diameter d_1 of the first layer near the core to optimize dispersion and nonlinear properties [2, 3]. The filling factor d_2/Λ is kept fixed at 0.95 while d_1/Λ is varied from 0.3 to 0.65 with the step of 0.5. The circular core is doped with a 10% molar concentration of GeO_2, whose diameter is determined by the formula $D_c = 2\Lambda - d_1$. The core diameter of the PCFs is also one of the important structural parameters because the size of the core affects the ability to confine electromagnetic waves. There are two ways to design the core size of PCFs. First, the core of the PCFs should not be too small to make dispersion control easier by designing photonic cladding. Second, the cores of the PCFs are large enough to reasonably match the

PCF-mode field diameters with the telecommunication single mode fiber. SiO_2 and GeO_2 are introduced into the data by declaring the coefficients in the Sellmeier Eqs. (1, 2) [22, 23].

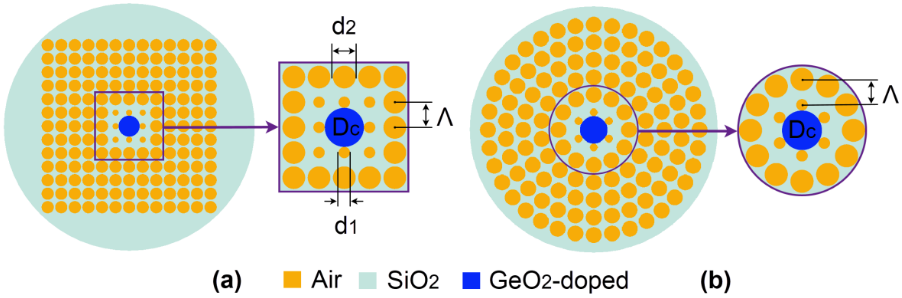

Figure 1. Cross-section view of the square (a) and circular (b) SiO_2-GeO_2 PCF.

With the full-vector finite-difference eigenmode method, the optical properties of the fibers in the 0.6 – 2.0 µm wavelength range are calculated by solving the Maxwell wave equation with the boundary condition which is perfectly matched layer rectangles. This helps to well absorb incoming waves from the computed region without any reflections. The light is well confined in the core of PCFs thanks to the reasonable adjustment of the doped GeO_2 molar concentration and lattice parameters (Fig. 2).

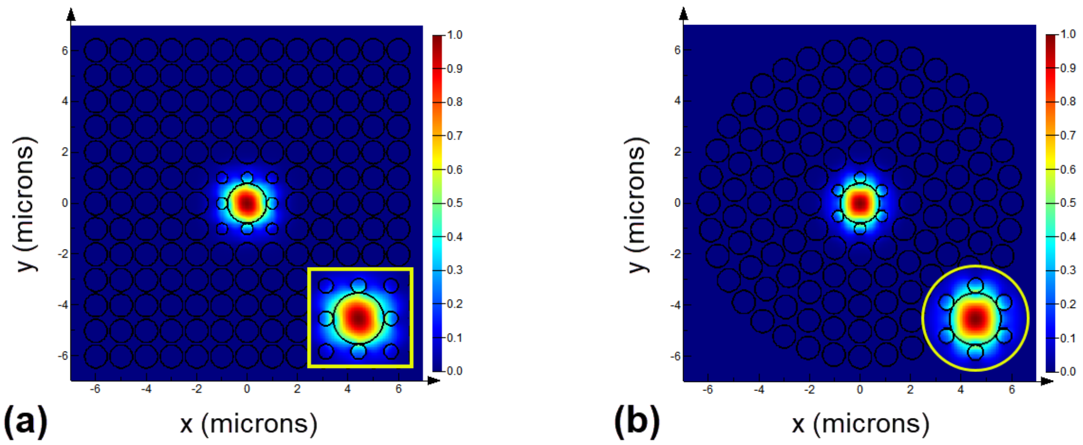

Figure 2. The light confinement in the core of the square (a) and circular (b) PCFs with Λ = 1.0 µm; d_1/Λ = 0.45.

$$n(\lambda) = \sqrt{1 + \sum_{i=1}^{3} \frac{B_i \lambda^2}{\lambda^2 - C_i^2}} \quad (1)$$

$$n_{(GeO_2\text{-}SiO_2)}(\lambda) = \sqrt{1 + \sum_{i=1}^{3} \frac{[SB_i + X(GB_i - SB_i)]\lambda^2}{\lambda^2 - [SC_i + X(GC_i - SC_i)]^2}} \quad (2)$$

where SB, SC, GB, and GC are the Sellmeier coefficients for the SiO_2 and GeO_2 glasses, respectively, and X is the mole fraction of GeO_2 (X = 0.1) (Table 1).

Table 1. Sellmeier's coefficients for the GeO_2-doped [23]

Parameters	SiO_2	GeO_2	GeO_2-doped
B_1	0.6961663	0.80686642	0.707236312
B_2	0.4079426	0.71815848	0.438964188
B_3	0.8974794	0.85416831	0.893148291
C_1 (μm)	6.84043×10^{-2}	6.8972606×10^{-2}	6.8461131×10^{-2}
C_2 (μm)	1.162414×10^{-1}	1.5396605×10^{-1}	1.20013865×10^{-1}
C_3 (μm)	9.896161	11.841931	10.090738

The refractive index of pure SiO_2, pure GeO_2 and a composite of 90% SiO_2 :10% GeO_2 with wavelength dependence are illustrated in Fig. 3. Pure GeO_2-based PCFs often exhibit a significant loss [10], although their refractive index is the largest in the investigated wavelength range. Therefore, the new structure of PCFs with a GeO_2 doped core with a specific molar concentration will help to reduce the loss and control the dispersion and the nonlinear properties of the PCFs, i.e. improve the SC generation efficiency. However, the GeO_2 doping rate should also be kept in mind since the loss of PCFs will increase as the GeO_2 doping concentration increases.

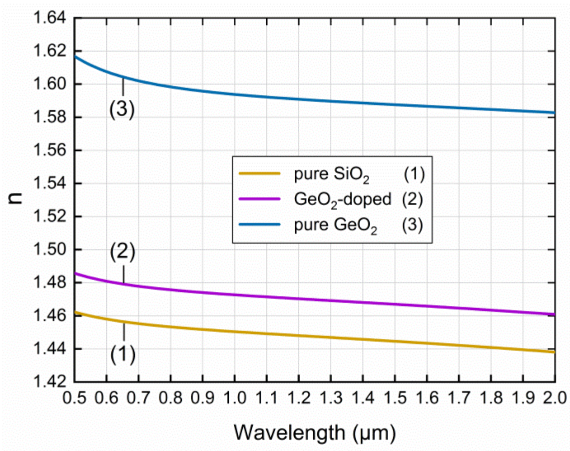

Figure 3. The effective refractive index real parts (n) of pure SiO_2, pure GeO_2, and composite SiO_2-GeO_2.

3. Simulation Results and Analysis

We only analyze dispersion for the fundamental mode of the optical fiber, because the effects of intermodal dispersion usually overshadow those of chromatic dispersion. Furthermore, when the input pulse is short enough (≤ 10 ps), the higher-order modes do not affect the SC spectral expansion much [24]. Dispersion is an important property of PCFs that determines the appearance of nonlinear effects during SC generation, and it characterizes the propagation with different velocities of the spectral components. Chromatic dispersion *(D)* includes material dispersion and waveguide dispersion, which is defined by following formula [9]:

$$D(\lambda) = -\frac{\lambda}{c}\frac{d^2\,\mathrm{Re}[n_{\mathrm{eff}}]}{d\lambda^2} \tag{3}$$

where λ and c are the wavelengths and the speed of light in a vacuum, respectively, and Re[n_{eff}] is the real part of the effective index of the guided mode.

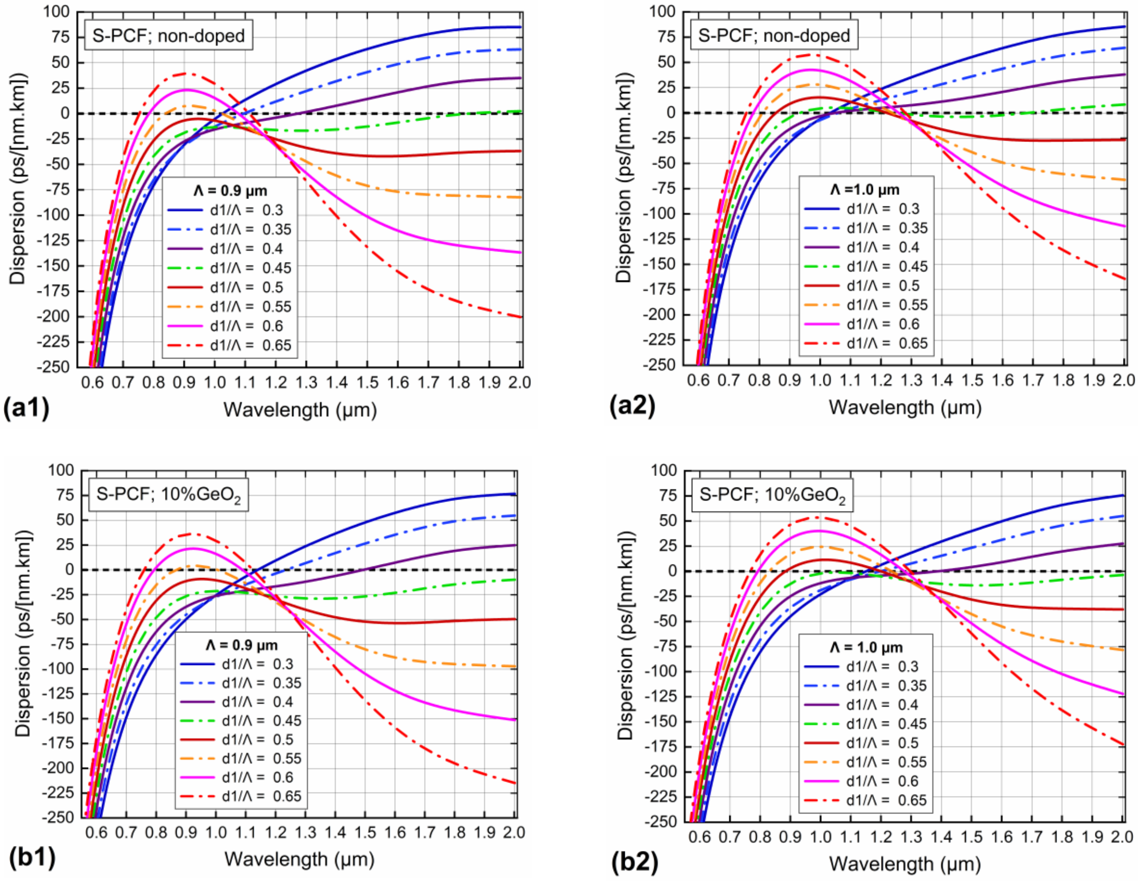

Figure 4. The chromatic dispersion characteristics of the square SiO_2-PCFs (a1 and a2) and composite SiO_2-GeO_2 PCFs (b1 and b2) with various values of d_1/Λ and Λ = 0.9 µm and 1.0 µm.

The variation of lattice parameters such as Λ and d_1/Λ governs the PCFs' dispersion properties and zero dispersion wavelength (ZDWs) shifts (Fig. 4). The dispersion properties are quite diverse with all-normal and anomalous dispersion. To further analyze the influence of GeO_2 doping on the dispersion properties of the fibers, we compare the dispersion of the undoped and doped square lattice fibers with the 10% molar concentration of GeO_2. In the case of Λ = 0.9 µm (Fig. 4a1), we obtain only fiber with all-normal dispersion with d_1/Λ = 0.5. The flattest anomalous dispersion with d_1/Λ = 0.45 (the green curve) intersects the zero dispersion at about 1.85 µm. When the fibers are doped with GeO_2 (Fig. 4b1), this curve becomes an all-normal dispersion curve, i.e. two all-normal dispersions are obtained with d_1/Λ = 0.45 and d_1/Λ = 0.5. It can be seen that doping GeO_2 can cause the value of dispersion to decrease, even to negative values in the wavelength range from 1.1 µm to 2.0 µm. SC generation applications with small dispersion values can perfectly accommodate these dispersions. More, the shift of the ZDW towards the longer wavelength is an essential factor for choosing the right pump wavelength in the SC generation, which is usually chosen close to the 1.55 µm wavelength. It is the wavelength at which SiO_2 materials exhibit the lowest loss, and is the wavelength of common lasers in practice. Comparing the dispersion curves in Figs. 4a1 and 4b1, the ZDWs tend to shift towards the longer wavelength when the core of the PCF is doped with GeO_2. Especially the dispersion curve with $d_1/\Lambda = 0.4$ has a ZDW of 1.493 µm which is closer to 1.55 µm. This structure is well suited for SC generation in the anomalous dispersion region with soliton dynamics being the main mechanism in spectral expansion.

When Λ is larger (Figs. 4a2 and 4b2), the number of all-normal dispersion curves is reduced. In the case of GeO_2 undoped PCFs, only anomalous dispersion curves are found, the ZDWs are very far from the wavelength of 1.55 µm. A flat all-normal dispersion curve with $d_1/\Lambda = 0.45$ is achieved when the fibers are doped with GeO_2 (Figure 4b2). This fiber is expected to generate SC in the all-normal dispersion region with nonlinear effects such as self-phase modulation and optical wave breaking.

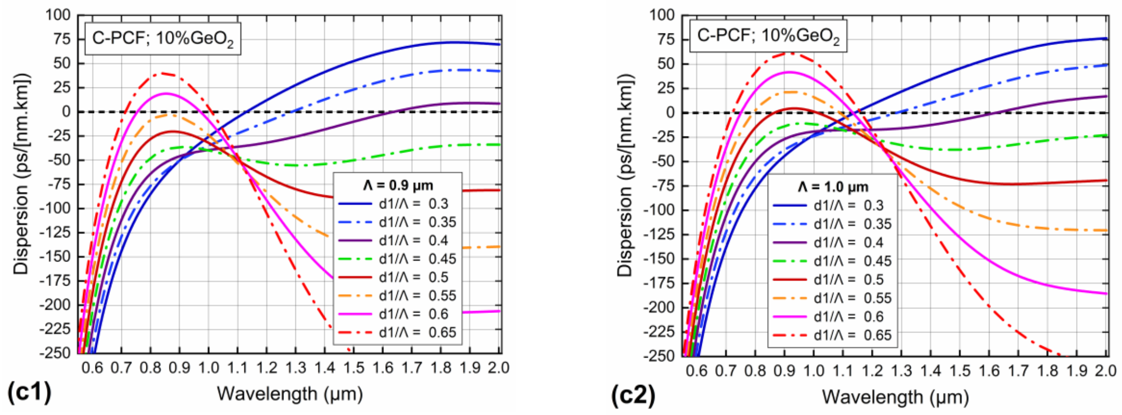

Figure 5. The chromatic dispersion characteristics of the circular composite SiO_2-GeO_2 PCFs with various values of d_1/Λ and Λ = 0.9 µm (c1) and 1.0 µm (c2).

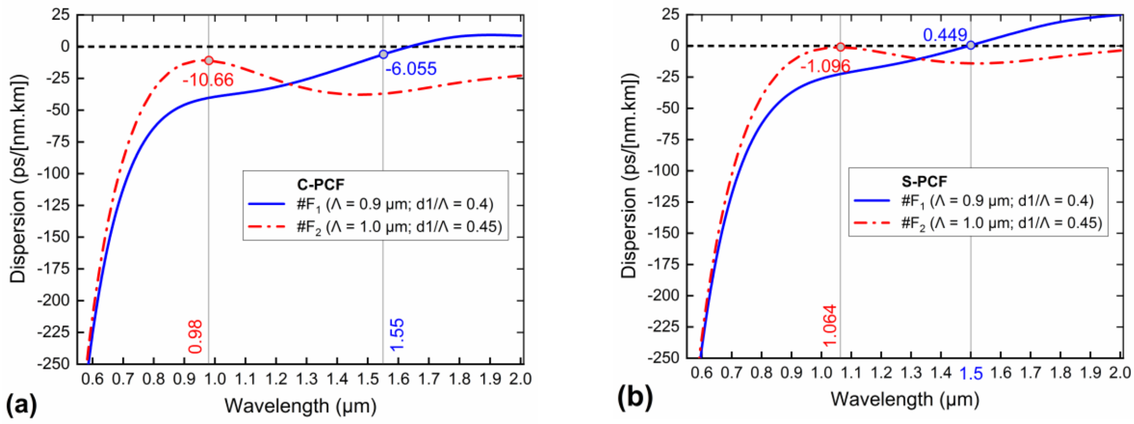

Figure 6. The chromatic dispersion characteristics of two proposed PCFs with circular (a) and square (b) lattice.

The dispersion properties of PCFs are also affected by the lattice types. With the same 10 mol% of doped GeO_2, we investigate the dispersion properties in circular lattice fibers (C-PCFs). The variation of dispersion curves with wavelength and lattice parameters are shown in Fig. 5. Compared with the square lattice PCFs (S-PCFs) (Fig. 4), the dispersion curves of the circular lattice PCFs are less flat and the ZDWs shift towards the longer wavelength. We chose PCFs with Λ = 0.9 µm, d_1/Λ = 0.4 (#F_1) and Λ = 1.0 µm, d_1/Λ = 0.45 (#F_2) which have circular and square lattice respectively for analysis and comparison dispersion properties (Fig. 6).

The anomalous dispersion of #F_1 with C-PCF is flatter, closer to the zero-dispersion line than that of S-PCF. However, the #F_1 fiber of S-PCF has a dispersion value of 0.449 ps/(nm.km) at a pump wavelength of 1.5 µm, which is smaller than that of the C-PCF fiber. The pump wavelength is chosen to satisfy two conditions: Firstly, it should be close to the maximum value of the dispersion curves to obtain a small value, which is convenient for SC application. Secondly, it must be suitable for the pump wavelength of laser sources in practice or other publications. With the all-normal dispersion of the S-CF, the #F_2 fiber has a flatter dispersion than that of the C-PCF. This dispersion curve is very close to zero-dispersion. Furthermore, dispersion values at the pump wavelength of 1.064 µm as small as −1.096 ps/(nm.km) are found. Based on the above numerical analysis, we propose two optimal structures of square lattice to simulate nonlinear properties and evaluate the suitability of these two fibers for SC orientation. The dispersion values obtained at the pump wavelength of the two proposed S-PCF fibers are smaller than some previous work on PCF based on SiO_2-GeO_2 composite [15, 17].

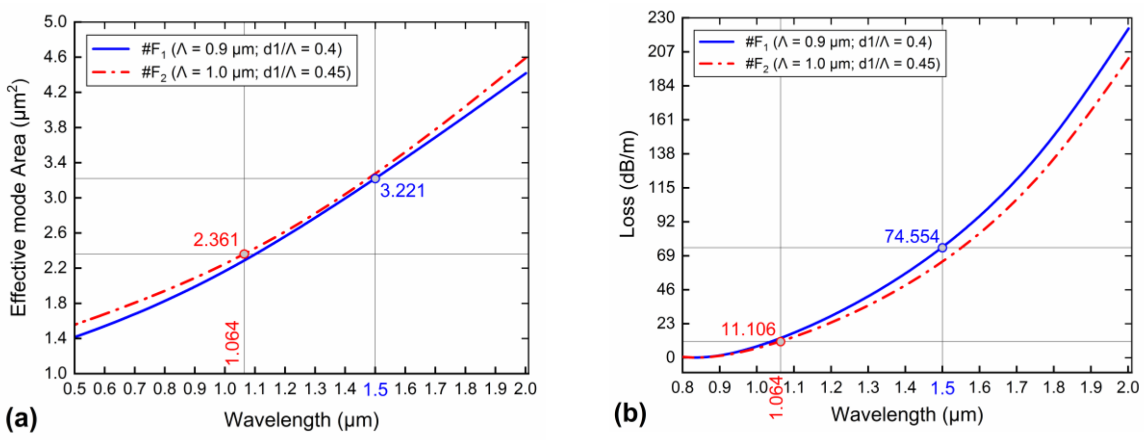

Figure 7. The effective mode area (a) and loss (b) of the two proposed S-PCF structures.

The effective area is an important fiber parameter because it determines how tightly the light is confined to the core and relates to the nonlinear effect in the fiber through the nonlinear coefficient. It is calculated by following formula [25]:

$$A_{\text{eff}} = \frac{\left(\int_{-\infty}^{\infty}\int_{-\infty}^{\infty} |E|^2 \, dxdy\right)^2}{\int_{-\infty}^{\infty}\int_{-\infty}^{\infty} |E|^4 \, dxdy} \tag{4}$$

where E is the amplitude of the transverse electric field propagating inside the PCF.

The nonlinear coefficient is inversely proportional to the effective mode area and is computed using the nonlinear refractive index for SiO_2-GeO_2 material n_2, as follows [25].

$$\gamma(\lambda) = 2\pi \frac{n_2}{\lambda A_{\text{eff}}} \tag{5}$$

The confinement loss characterizes the gradual decrease in power with propagation distance as light propagates in an optical fiber. It depends on the wavelength and the imaginary part of the effective refractive index, which is defined by following formula [26]:

$$L_c = 8.686 \frac{2\pi}{\lambda} \mathrm{Im}[n_{\mathrm{eff}}(\lambda)] \quad (6)$$

The graphs of effective mode area and loss vs wavelength for two proposed S-PCF structures are shown in Fig. 7. The effective mode area increases with increasing wavelength. The low-frequency waves have difficulty entering the core region of the PCF, leading to leakage of modes into the cladding or between different air holes, which causes an increase in A_{eff} in this wavelength region. The effective mode area of #F_2 fiber is larger than that of #F_1 fiber in the investigated wavelength range because #F_2 fiber has a larger core diameter than #F_1. The larger the core size fibers, the less likely they are to confine light to the core. The effective mode area at the pump wavelength of the two fibers #F_1 and #F_2 is 3.221 μm^2 and 2.361 μm^2, respectively. #F_2 fiber has a smaller effective mode area at the pump wavelength, i.e. a larger nonlinear coefficient. The nonlinear coefficients at the pumping wavelength of #F_1 and #F_2 fibers are also calculated. They are 32.49 $W^{-1}.km^{-1}$ and 62.387 $W^{-1}.km^{-1}$, respectively. These values are similar to the nonlinear coefficient reported in [15] and much larger than that as shown in [17]. The confinement loss of the two proposed fibers increases quite rapidly in the 1.6−2.0 µm wavelength region, which is consistent with the loss of silica substrate in this wavelength range. The values of L_c at the pump wavelength of two fibers #F_1 and #F_2 are 74.554 dB/m and 11.106 dB/m. Although the L_c value obtained in our work is larger than previous publications [12, 16], the fibers exhibit flat dispersion, a small dispersion value, and a high nonlinear coefficient suitable for the SC application. It should also be noted that it is difficult to simultaneously optimize the optical properties of PCFs. Depending on different application purposes, it may be preferable to optimize the specific properties of PCF.

4. Conclusion

GeO_2 doping in silica-based PCFs and suitable modification of lattice parameters are demonstrated as the essential factors for optimizing dispersion and other nonlinear properties of optical fiber, which strongly govern SC spectral characteristics. We compared dispersion based on designed PCFs with square, circular, doped, and undoped GeO_2 lattices to evaluate the optimality in dispersion. From this, we introduce two optimized square lattice structures based on PCF doped 10 mol% of GeO_2 for detailed analysis of dispersion and other nonlinear properties, including effective mode area, nonlinear coefficients, and confinement loss. The anomalous and all-normal flat dispersion of the #F_1 and #F_2 fibers help to diversify the spectral characteristics in SC generation applications. The small dispersion values of 0.449 ps/(nm.km) and −1.096 ps/(nm.km), which are the outstanding advantage of this work, will help to broaden the SC spectrum. The low peak power laser pump sources in SC application will be suitable when using fibers with large nonlinear coefficients of 32.49 $W^{-1}.km^{-1}$ and 62.387 $W^{-1}.km^{-1}$, such as #F_1 and #F_2.

References

[1] X. Zou, T. Izumitani, Spectroscopic Properties and Mechanisms of Excited State Absorption and Energy Transfer Upconversion for Er^{3+}-Doped Glasses, Journal Non-Crystalline Solids, Vol. 162, No. 1-2, 1993, pp. 68-80, https://doi.org/10.1016/0022-3093(93)90742-G.

[2] L. C. Van, T. N. Thi, D. H. Trong, B. T. L. Tran, N. V. T. Minh, T. V. Dang, T. L. Canh, Q. H. Dinh, K. D. Quoc, Comparison of Supercontinuum Spectrum Generating by Hollow Core PCFs Filled with Nitrobenzene with Different Lattice Types, Optical and Quantum Electronics, Vol. 54, 2022, pp. 300, https://doi.org/10.1007/s11082-022-03667-y.

[3] T. N. Thi, D. H. Trong, B. T. L. Tran, T. D. Van, L. C. Van, Optimization of Optical Properties of Toluene-Core Photonic Crystal Fibers with Circle Lattice for Supercontinuum Generation, Journal of Optics, 2022, https://doi.org/10.1007/s12596-021-00802-y.

[4] L. C. Van, V. T. Hoang, V. C. Long, K. Borzycki, K. D. Xuan, V. T. Quoc, M. Trippenbach, R. Buczyński, J. Pniewski, Supercontinuum Generation in Benzene-Filled Hollow-Core Fibers, Optical Engineering, Vol. 60, No. 11, 2021, pp. 116109, https://doi.org/10.1117/1.OE.60.11.116109.

[5] H. Q. Quy, C. V. Lanh, Spectrum Broadening of Supercontinuum Generation by Fill Styrene in Core of Photonic Crystal Fibers, Indian Journal of Pure & Applied Physics, Vol. 59, 2021, pp. 522-527.

[6] B. T. L. Tran, T. N. Thi, N. V. T. Minh, T. L. Canh, M. L. Van, V. C. Long, K. D. Xuan, L. C. Van, Analysis of Dispersion Characteristics of Solid-Core PCFs with Different Types of Lattice in The Claddings, Infiltrated with Ethanol, Photonics Letters of Poland, Vol. 12, No. 4, 2020, pp. 106-108, https://doi.org/10.4302/plp.v12i4.1054.

[7] C. V. Lanh, V. T. Hoang, V. C. Long, K. Borzycki, K. D. Xuan, V. T. Quoc, M. Trippenbach, R. Buczyński, J. Pniewski, Supercontinuum Generation in Photonic Crystal Fibers Infiltrated with Nitrobenzene, Laser Physics, Vol. 30, 2020, pp. 035105-035109, https://doi.org/10.1088/1555-6611/ab6f09.

[8] C. V. Lanh, V. T. Hoang, V. C. Long, K. Borzycki, K. D. Xuan, V. T. Quoc, M. Trippenbach, R. Buczyński, J. Pniewski, Optimization of Optical Properties of Photonic Crystal Fibers Infiltrated with Chloroform for Supercontinuum Generation, Laser Physics, Vol. 29, No. 7, 2019, pp. 075107, https://doi.org/10.1088/1555-6611/ab2115.

[9] Y. S. Lee, C. G. Lee, F. Bahloul, S. Kim, K. Oh, Simultaneously Achieving a Large Negative Dispersion and a High Birefringence over Er and Tm Dual Gain Bands in a Square Lattice Photonic Crystal Fiber, Journal of Lightwave Technology, Vol. 37, No. 4, 2019, pp. 1254-1263, https://doi.org/10.1109/JLT.2019.2891756.

[10] P. H. Reddy, A. V. Kir'yanov, A. Dhar, S. Das, D. Dutta, M. Pal, Y. O. Barmenkov, J. A. M. Gallardo, S. K. Bhadra, M. C. Paul, Fabrication of Ultra-High Numerical Aperture GeO_2-Doped Fiber and Its Use for Broadband Supercontinuum Generation, Applied Optics, Vol. 56, No. 33, 2017, pp. 9315-9324, https://doi.org/10.1364/AO.56.009315.

[11] L. Yang, B. Zhang, K. Yin, J. Yao, G. Liu, J. Hou, 0.6-3.2 μm Supercontinuum Generation in a Step-Index Germania-Core Fiber Using a 4.4 kW Peak-Power Pump Laser, Optics Express, Vol. 24, No. 12, 2016, pp. 12600-12606, https://doi.org/10.1364/OE.24.012600.

[12] B. A. Cumberland, S. V. Popov, J. R. Taylor, O. I. Medvedkov, S. A. Vasiliev, E. M. Dianov, 2.1 microm Continuous-Wave Raman Laser in GeO_2 Fiber, Optics Letters, Vol. 32, No. 13, 2007, pp. 1848-1850, https://doi.org/10.1364/OL.32.001848.

[13] D. Michalik, T. Stefaniuk, R. Buczynski, Dispersion Management in Hybrid Optical Fibers, Journal of Lightwave Technology, Vol. 38, No. 6, 2020, pp. 1427-1434, https://doi.org/10.1109/JLT.2019.2952250.

[14] J. Liaoa, Z. Wang, T. Huang, Q. Wei, D. Li, Design of Step-Index-Microstructured Hybrid Fiber for Coherent Supercontinuum Generation, Optik, Vol. 243, 2021, pp. 167393, https://doi.org/10.1016/j.ijleo.2021.167393.

[15] M. A. Hossain, Y. Namihira, M. A. Islam, Y. Hirako, Polarization Maintaining Highly Nonlinear Photonic Crystal Fiber for Supercontinuum Generation at 1.55 µm, Optics & Laser Technology, Vol. 44, No. 5, 2012, pp. 1261-1269, https://doi.org/10.1016/j.optlastec.2011.12.052.

[16] A. A. Nair, I. S. Amiri, C. S. Boopathi, S. Karthikumar, M. Jayaraju, P. Yupapin, Numerical Investigation of Co-Doped Microstructured Fiber with Two Zero Dispersion Wavelengths, Results in Physics, Vol. 10, 2018, pp. 766-771, https://doi.org/10.1016/j.rinp.2018.07.032.

[17] Y. K. Prajapati, V. K. Srivastava, V. Singh, J. P. Sainid, Effect of Germanium Doping on The Performance of Silica Based Photonic Crystal Fiber, Optik, Vol. 155, 2018, pp. 149-156, https://doi.org/10.1016/j.ijleo.2017.10.178.

[18] J. C. Vinda, S. T. Peiró, A. Diez, M. V. Andrés, Supercontinuum Generation in Highly Ge-Doped Core Y-Shaped Microstructured Optical Fiber, Applied Physics B, Vol. 98, 2010, pp. 371-376, https://doi.org/10.1007/s00340-009-3723-5.

[19] J. Yang, Y. Wang, Y. Fang, W. Geng, W. Zhao, C. Bao, Y. Ren, Z. Wang, Y. Liu, Z. Pan, Y. Yue, Over-Two-Octave Supercontinuum Generation of Light-Carrying Orbital Angular Momentum in Germania Doped Ring-Core Fiber, Sensors, Vol. 22, No. 17, 2022, pp. 6699, https://doi.org/10.3390/s22176699.

[20] H. Chen, H. Wei, T. Liu, X. Zhou, P. Yan, Z. Chen, S. Chen, J. Li, J. Hou, Q. Lu, All-Fiber-Integrated High-Power Supercontinuum Sources Based on Multi-Core Photonic Crystal Fibers, IEEE Journal of Selected Topics in Quantum Electronics, Vol. 20, No. 5, 2014, pp. 64-71, https://doi.org/10.1109/JPHOT.2011.2175211.

[21] D. Jain, R. Sidharthan, P. M. Moselund, S. Yoo, D. Ho, O. Bang, High Power, Ultra-Broadband Supercontinuum Source Based on Highly GeO_2 Doped Silica Fiber, Fiber Lasers XIV: Technology and Systems, Vol. 10083, 2017, pp. 1008318, https://doi.org/10.1117/12.2251648.

[22] I. H. Malitson, Interspecimen Comparison of The Refractive Index of Fused Silica, Journal of the Optical Society of America, Vol. 55, No. 10, 1965, pp. 1205-1208, https://doi.org/10.1364/JOSA.55.001205.

[23] J. W. Fleming, Dispersion in GeO_2-SiO_2 Glasses, Applied Optics, Vol. 23, No. 24, 1984, pp. 4486-4493, https://doi.org/10.1364/AO.23.004486.

[24] I. Kubat, O. Bang, Multimode Supercontinuum Generation in Chalcogenide Glass Fibres, Optics Express, Vol. 24, No. 3, 2016, pp. 2513-2526, https://doi.org/10.1364/OE.24.002513.

[25] G. P. Agrawal, Nonlinear Fiber Optics (5^{th} edition), Elsevier, Amsterdam, 2013, https://doi.org/10.1016/C2011-0-00045-5.

[26] C. Wei, H. Zhang, H. L. Hongxi, S. Y. Liu, Broadband Mid-Infrared Supercontinuum Generation Using a Novel Selectively Air-Hole Filled As_2S_5-As_2S_3 Hybrid PCF, Optik, Vol. 141, 2017, pp. 32-38, https://doi.org/10.1016/j.ijleo.2017.02.061.